Efficient coupler between chip-level and board-level optical waveguides

Jie Shu, Ciyuan Qiu, Xuezhi Zhang, and Qianfan Xu*

Department of Electrical and Computer Engineering, Rice University, Houston, Texas 77005, USA
**Corresponding author: qianfan@rice.edu*

Received July 27, 2011; revised August 18, 2011; accepted August 18, 2011;
posted August 19, 2011 (Doc. ID 151547); published September 13, 2011

We propose an efficient optical coupler between a submicrometer-sized silicon waveguide on a silicon photonic chip and a multi-micrometer wide polymer waveguide on an optical printed circuit board for interchip optical networks. We show low coupling loss <0.4 dB with high lateral and angular tolerance to misalignment so that coupling can be done by automatic pick-and-place equipments with high throughput and low cost. The coupler has a wide optical bandwidth from 1470 to 1650 nm. © 2011 Optical Society of America

OCIS codes: 230.7370, 130.5460, 130.5990.

With the recent development in silicon photonics, large-scale optical interconnection networks based on silicon waveguides can be monolithically integrated on many-core chips to provide high-bandwidth and low-power-consumption communications between the cores [1–4]. For interchip links, low-loss polymer waveguides that are compatible with the printed circuit board have been developed [5–7]. Efficient coupling between these two types of waveguides is challenging due to their large difference in cross-sectional dimensions.

Here we propose an efficient coupler based on a silicon nanotaper that can couple light between a submicrometer sized silicon waveguide on chip and a multi-micrometer wide polymer waveguide on board. We show a low coupling loss of 0.4 dB that is tolerant to a lateral misalignment as large as the width of the polymer waveguide. The coupling process is compatible with existing electronic chip-to-board assembly technologies. Such a coupler makes an optical interconnection network nearly blind to chip boundaries, a tremendous advantage compared to electronic interconnects, where off-chip links are much slower and much more power hungry.

Figure 1 shows the structure of this coupler. It consists of a silicon nanotaper flip-chip bonded on top of a polymer waveguide. The flip-chip bonding process is one of the standard processes for chip packaging [8]. When the proposed optical couplers, which act as optical pins, are integrated into the process, electrical connections and optical connections can be made at one step. Moreover, this nanotaper-based coupling scheme can be scaled to a large coupler array spanning the edge of the chip, which can be coupled simultaneously, while each connection can support data bandwidth on the order of Tbit/s [9,10].

Silicon can confine light tightly in a waveguide with cross-sectional dimensions much smaller than the wavelength of light because of its high refractive index. The commonly used silicon waveguide, built on top of silicon-on-insulator substrates, is around a half micrometer wide and a quarter micrometer tall. This type of waveguide can bend light tightly with a radius comparable to the wavelength [11], which is an important feature to achieve large-scale photonic integration. The small size, however, makes it difficult to couple directly to larger off-chip waveguides. The polymer waveguides on board normally have a width of several micrometers.

To couple to the wider polymer waveguide, the width of the silicon waveguide can be further shrunk to ~0.1 μm with a nanotaper structure [12]. In the taper, the optical mode becomes delocalized when the width is too small to support a highly confined mode. When this nanotaper is placed close to a polymer waveguide with refraction index higher than that of SiO_2, the delocalized optical field will gradually transit into the core of the polymer waveguide, resulting in a low-loss coupling between the two waveguides with dramatically different dimensions. Given the fact that this coupling scheme requires only proximity between the nanotaper and the polymer waveguide, not specific position relationships, it has high tolerance to alignment error between the two structures.

The propagation of optical waves in the coupling structure is simulated based on the eigenmode expansion method [13]. The input is set as the fundamental TE mode of the silicon waveguide, and the output is the fundamental TE mode of the polymer waveguide. In order to simulate the coupling process, the taper is divided into many sections along the propagation axis. At the interface between two sections, the transfer matrix is computed based on the overlap between the modes in the two sections [13]. Besides the confined TE mode, TM modes and radiation modes are also included in the computation.

Figure 2(a) shows the top-view field distributions in the coupler when the nanotaper is perfectly aligned with the polymer waveguide. As the width of the silicon

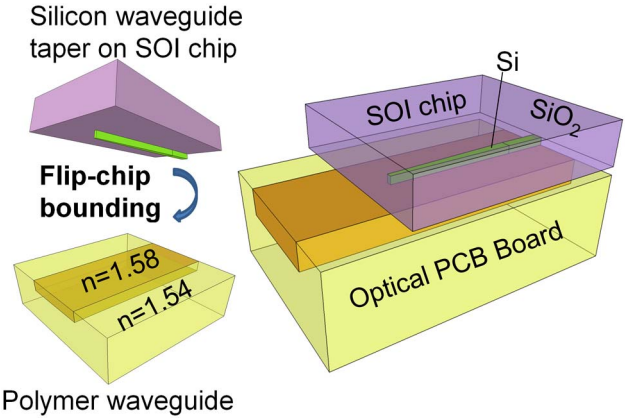

Fig. 1. (Color online) Schematics of the proposed coupler.

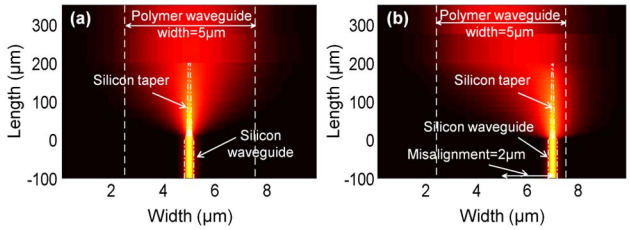

Fig. 2. (Color online) Distribution of the H field as light adiabatically couples from a 0.45 μm wide and 0.25 μm high silicon waveguide to a 5 μm wide and 1.25 μm high polymer waveguide with SU-8 ($n = 1.58$) core and NOA61 ($n = 1.54$) cladding [14]. (a) silicon taper is aligned with the center of the polymer waveguide. (b) silicon taper is misaligned by 2 μm with respect to the center of the polymer waveguide.

waveguide shrinks along the taper, light gradually transits into the wider polymer waveguide. When the silicon taper ends, over 94% of the optical wave continues to propagate in polymer waveguide, corresponding to an insertion loss of only 0.27 dB. Because of the nature of the adiabatic coupling, if the silicon waveguide is misaligned with the center of the polymer waveguide, the optical field automatically shifts toward the center of the polymer waveguide when it is delocalized from the silicon, which is shown in Fig. 2(b). Therefore, the coupling coefficient remains high as long as the silicon waveguide lies within or close to the polymer waveguide.

Figure 3 shows the simulated coupling efficiency versus misalignment for a 5 μm wide and a 12 μm wide polymer waveguide. When coupled to the 5 μm wide waveguide, the coupling loss is below 0.4 dB for any misalignment within ± 2.5 μm. This 5 μm range for low-loss coupling is 11 times the width of the highly confined silicon waveguide. This alignment tolerance, while not as high as that for electrical connection, exceeds the placement accuracy of some commercial automatic flip-chip bonders. The capability of performing optical coupling

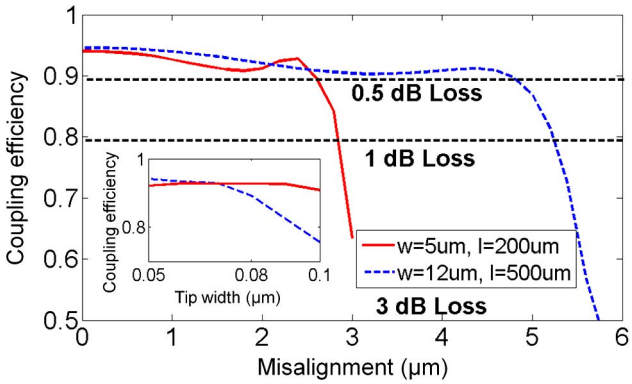

Fig. 3. (Color online) Coupling efficiency of the coupler versus the lateral misalignment between the silicon nanotaper and polymer waveguide center. Red solid line: a 200 μm long nanotaper with 0.1 μm wide taper tip coupled to a 5 μm wide polymer waveguide. Blue dashed line: a 500 μm long nanotaper with 0.05 μm wide taper tip coupled to a 12 μm wide polymer waveguide. The inset shows coupling efficiency versus the tip width of the silicon taper. Red solid line: a 200 μm long nanotaper coupled to a 5 μm wide polymer waveguide with a 2 μm misalignment. Blue dashed line: a 500 μm long nanotaper coupled to a 12 μm wide polymer waveguide with a 3.8 μm misalignment.

passively with standard equipments will bring the cost of optoelectronic packaging and assembly in line with their electrical counterpart.

If an even larger misalignment tolerance is required for a low cost coupling system, a wider polymer waveguide can be used. A 12 μm wide polymer waveguide can extend the misalignment tolerance to ± 5 μm. The tradeoff is that a nanotaper with a longer length (500 μm) and a narrower tip is needed. A longer taper length is required because the angle of field expansion is limited by the condition for adiabatic transition. The inset of Fig. 3 shows that the taper tip needs to be narrower when coupling to a wider polymer waveguide.

The shape of the taper is critical in determining the taper length that is needed to achieve a given coupling efficiency. To minimize the taper length, we first identified that the main loss mechanism of the coupler is the coupling to the second-order TE mode (which is a radiation mode in the single-mode waveguide). Couplings to other higher order modes such as the third-order TE mode are much lower, as shown in Fig. 4(a). For a linear shaped taper, the loss from coupling to the second-order TE mode is high when the taper is short and when the misalignment is large, but most of this coupling happens in a small portion of taper, as shown in Fig. 4(b). Therefore, we can minimize the loss with low impact on the overall length of the taper by extending only the taper sections that cause high coupling to the second-order mode. We optimize the taper shape by making the slope of the taper inversely proportional to the coupling coefficient to the second-order TE mode at that taper section. A 200 μm long taper designed this way is shown in Fig. 4(c). With this approach, the required taper length for <0.5 dB coupling loss is significantly reduced to 100 μm from 400 μm for linear shaped taper as shown in Fig. 4(d). The lines plotted in Fig. 3 are based on this optimized taper shapes.

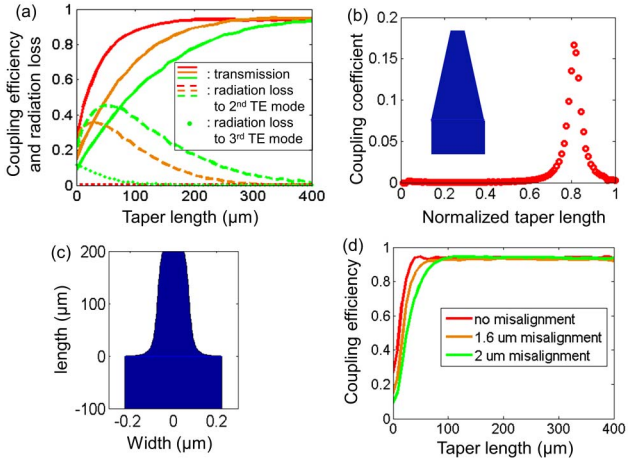

Fig. 4. (Color online) Design of taper shape. (a) Linear taper: coupling efficiency (solid), loss to second-order TE mode (dashed) and loss to third-order TE mode (dotted) versus the taper length. Red: no misalignment. Brown: 1.6 μm misalignment. Green: 2 μm misalignment. (b) Coupling coefficient from the fundamental TE mode to the second-order TE mode at different posistion along the taper. (c) The optimized taper shape (d) Coupling efficiency for the taper with the optimized shape versus the taper length. Red (darkest): no misalignment. Brown: 1.6 μm misalignment. Green (lightest): 2 μm misalignment.

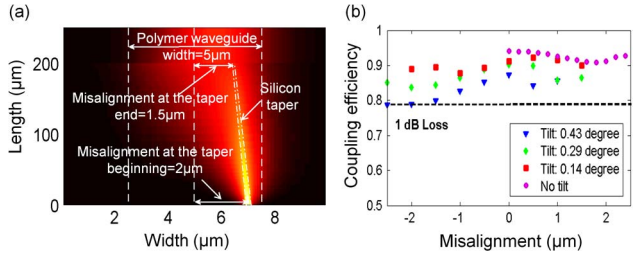

Fig. 5. (Color online) (a) Distribution of the H field when the misalignment between the silicon taper and the center of the polymer waveguide changes from $2\,\mu$m at the beginning of the taper to $1.5\,\mu$m at the tip of the taper (b) Coupling efficiency versus misalignment at the taper tip for different tilt angles.

The strength of coupling to the second-order mode at each taper section varies with the misalignment between taper and polymer waveguide. We can only use the data for one particular misalignment to design the taper shape that minimizes the loss for that particular misalignment. For the $5\,\mu$m wide waveguide, we minimize the loss for a misalignment of $2.4\,\mu$m, so the transmission curve (the red solid line in Fig. 3) shows a local maximum at that misalignment.

During flip-chip bonding process of the silicon and polymer waveguides, besides the lateral misalignment of these two waveguides, there is possibly angular misalignment. We investigate the situation when the propagation axes of the two waveguides are not parallel, as shown in Fig. 5(a). When simulating optical propagation in the nanotaper sections, the propagation axis is fixed along the direction of the taper instead of along the polymer waveguide because the light is mainly inside the taper. At the end of the taper, the light starts to propagate along the polymer waveguide, where we project the field amplitude onto the cross section of the polymer waveguide with a proper account of the phase distribution. Figure 5(b) shows the effect on transmission of the coupler for such angular misalignment. The taper tilting is assumed to be from right to left, and the misalignment is defined as the displacement between the taper end and the center of polymer waveguide. With an angular misalignment as large as 0.43°, the coupling loss remains below 1 dB as long as the tip of the silicon nanotaper lies within the width of the polymer waveguide.

The adiabatic coupling scheme is inherently broadband. To show the optical bandwidth of the coupler, in Fig. 6 we plot the coupling efficiency at several different wavelengths from 1470 to 1650 nm. When the waveguide misalignment is small, the coupling efficiency does not change with wavelength. With larger misalignment, since the shape of the taper is designed to minimize the radiation loss at the wavelength of 1550 nm, the radiation loss increases at wavelengths further away from 1550 nm. However, over the whole 180 nm wide optical band, the total coupling loss remains less than 1 dB for any misalignment within $\pm 2.5\,\mu$m.

In conclusion, we have proposed an efficient optical coupler between submicrometer sized silicon waveguides on chip and multi-micrometer wide polymer waveguides on board. Simulation results show low coupling loss <0.4 dB with large optical bandwidth and high tolerance to both lateral and angular misalignment. We show an approach to design the shape of the taper in order to minimize the taper length.

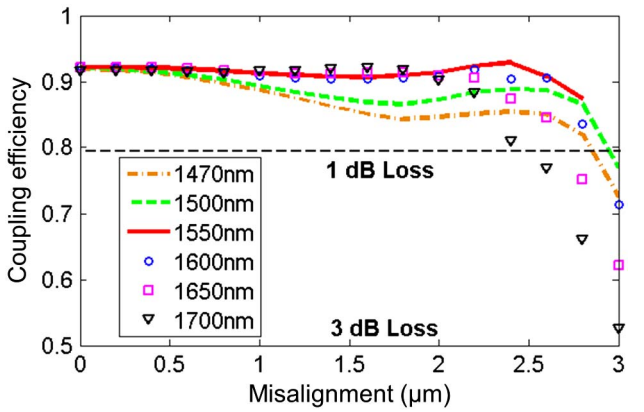

Fig. 6. (Color online) Coupling efficiency versus the lateral misalignment between the 200 nm long silicon nanotaper and $5\,\mu$m wide polymer waveguide center. Different colors and markers stand for different wavelengths.

References

1. J. Ahn, M. Fiorentino, R. G. Beausoleil, N. Binkert, A. Davis, D. Fattal, N. P. Jouppi, M. McLaren, C. M. Santori, R. S. Schreiber, S. M. Spillane, D. Vantrease, and Q. Xu, Appl. Phys. A **95**, 989 (2009).
2. A. Shacham, K. Bergman, and L. P. Carloni, IEEE Trans. Comput. **57**, 1246 (2008).
3. M. Petracca, K. Bergman, and L. P. Carloni, in *IEEE International Symposium on Circuits and Systems* (ISCAS, 2008), 2789.
4. C. Batten, A. Joshi, J. Orcutt, A. Khilo, B. Moss, C. Holzwarth, M. Popovic, L. Hanqing, H. Smith, J. Hoyt, F. Kartner, R. Ram, V. Stojanovic, and K. Asanovic, in *16th IEEE Symposium on High Performance Interconnects* (IEEE, 2008).
5. K. B. Yoon, I.-K. Cho, S. H. Ahn, M. Y. Jeong, D. J. Lee, Y. U. Heo, B. S. Rho, H.-H. Park, and B.-H. Rhee, J. Lightwave Technol. **22**, 2119 (2004).
6. R. Dangel, C. Berger, R. Beyeler, L. Dellmann, M. Gmur, R. Hamelin, F. Horst, T. Lamprecht, T. Morf, S. Oggioni, M. Spreafico, and B. J. Offrein, IEEE Trans. Adv. Packag. **31**, 759 (2008).
7. L. Eldada and L. W. Shacklette, J. Sel. Topics Quantum Electron. **6**, 54 (2000).
8. ESIA, JEITA, KSIA, TSIA, and SIA, "The international technology roadmap for semiconductors" (2007).
9. Q. Xu, S. Manipatruni, B. Schmidt, J. Shakya, and M. Lipson, Opt. Express **15**, 430 (2007).
10. Q. Xu, B. Schmidt, J. Shakya, and M. Lipson, Opt. Express **14**, 9430 (2006).
11. Q. Xu, D. Fattal, and R. G. Beausoleil, Opt. Express **16**, 4309 (2008).
12. V. R. Almeida, R. Panepucci and M. Lipson, Opt. Lett. **28**, 1302 (2003).
13. H. Wenzel, R. Güther, A. M. Shams-Zadeh-Amiri, and P. Bienstman, IEEE J. Quantum Electron. **42**, 64 (2006).
14. W. H. Wong, J. Zhou, and E. Y. B. Pun, Appl. Phys. Lett. **78**, 2110 (2001).